

RESEARCH ARTICLE

Comprehensive analysis of miRNA and protein profiles within exosomes derived from canine lymphoid tumour cell lines

Hajime Asada¹✉, Hirotaka Tomiyasu¹✉*, Takao Uchikai², Genki Ishihara², Yuko Goto-Koshino¹, Koichi Ohno¹, Hajime Tsujimoto¹

1 Department of Veterinary Internal Medicine, Graduate School of Agricultural and Life Sciences, The University of Tokyo, Bunkyo-ku, Tokyo, Japan, **2** Anicom Specialty Medical Institute Inc., Shinjuku-ku, Tokyo, Japan

✉ These authors contributed equally to this work.

* atomi@mail.ecc.u-tokyo.ac.jp

OPEN ACCESS

Citation: Asada H, Tomiyasu H, Uchikai T, Ishihara G, Goto-Koshino Y, Ohno K, et al. (2019) Comprehensive analysis of miRNA and protein profiles within exosomes derived from canine lymphoid tumour cell lines. *PLoS ONE* 14(4): e0208567. <https://doi.org/10.1371/journal.pone.0208567>

Editor: Yun Zheng, Kunming University of Science and Technology, CHINA

Received: November 16, 2018

Accepted: April 7, 2019

Published: April 29, 2019

Copyright: © 2019 Asada et al. This is an open access article distributed under the terms of the [Creative Commons Attribution License](https://creativecommons.org/licenses/by/4.0/), which permits unrestricted use, distribution, and reproduction in any medium, provided the original author and source are credited.

Data Availability Statement: The data from small RNA sequencing in this study are available in the DDBJ Sequenced Read Archive database with the accession number DRA006696 (<https://ddbj.nig.ac.jp/DRAsearch/submission?acc=DRA006696>).

Funding: This study was supported by the Japan Society for the Promotion of Science, KAKENHI [grant number 17H05043 and 17H03921]. Hirotaka Tomiyasu received 17H05043 and Hajime Tsujimoto received 17H03921. The funders had no

Abstract

Exosomes are small extracellular vesicles released from almost all cell types, which play roles in cell-cell communication. Recent studies have suggested that microenvironmental crosstalk mediated by exosomes is an important factor in the escape of tumour cells from the anti-tumour immune system in human haematopoietic malignancies. Here, we conducted comprehensive analysis of the miRNA and protein profiles within the exosomes released from four canine lymphoid tumour cell lines as a model of human lymphoid tumours. The results showed that the major miRNAs and proteins extracted from the exosomes were similar among the four cell lines. However, the miRNA profiles differed among the exosomes of each cell line, which corresponded to the expression patterns of the parent cells. In the comparison of the amounts of miRNAs and proteins among the cell lines, those of three miRNAs (miR-151, miR-8908a-3p, and miR-486) and CD82 protein differed between exosomes derived from vincristine-sensitive and resistant cell lines. Further investigations are needed to elucidate the biological functions of the exosomal contents in the microenvironmental crosstalk of lymphoid tumours.

Introduction

Exosomes are small extracellular vesicles released from almost all cell types, including immune cells and tumour cells [1], as the intracellular endosome component. Although exosomes were initially considered cellular waste, they have been shown to contain various molecules from the original cells, including proteins, functional mRNAs and miRNAs, and deliver these biological messages into the recipient cells [1,2]. To date, it has also been reported that tumour cells release a number of exosomes and they stimulate tumour cell growth and modify the immune cell response to promote tumour progression and metastasis in several human tumours, including colorectal cancer [3], breast cancer [4], melanoma [5], and pancreatic cancer [6]. Thus, the interaction between tumour cell-derived exosomes and recipient cells via both RNAs and proteins contained in exosomes in the microenvironment of solid tumours is

role in study design, data collection and analysis, decision to publish, or preparation of the manuscript. In addition, Anicom Specialty Medical Institute Inc. provided support in the form of salaries for authors [T.U. and G.I.], but did not have any additional role in the study design, data collection and analysis, decision to publish, or preparation of the manuscript. The specific roles of these authors are articulated in the 'author contributions' section.

Competing interests: Anicom Specialty Medical Institute Inc. provided support in the form of salaries for authors [T.U. and G.I.], but did not have any additional role in the study design, data collection and analysis, decision to publish, or preparation of the manuscript. This does not alter our adherence to PLOS ONE policies on sharing data and materials.

considered an important factor in tumour progression, metastasis, cell survival, and escape from the anti-tumour immune system.

Exosomes have also been suggested to play important roles in the microenvironmental crosstalk of human haematopoietic tumours, including leukaemia and lymphoma [7,8]. It has been reported that exosomes derived from acute/chronic myeloid leukaemia and lymphoma cells inactivate natural killer cells and suppress the anti-tumour immune response [7–9]. In addition, exosomes have been reported to be associated with drug resistance in these tumours [7]. For instance, it was reported that exosomes derived from imatinib-resistant chronic leukaemia cells could confer imatinib-resistance traits into sensitive cells by delivering miR-365 [10]. It was also reported that exosomes derived from bone marrow stromal cells decreased the sensitivity of acute lymphoblastic leukaemia cells to etoposide [11]. Based on these backgrounds, it has been considered that studies on the molecules contained in exosomes released from haematopoietic tumour cells could provide insight into the pathophysiology of these tumours. The profiles of miRNA and protein within exosomes were reported in virus-infected lymphoma cell lines [12,13] and lymphocytic leukaemia cells [14,15]. Although previous studies on molecules within exosomes have reported the biological functions of miRNAs or proteins in pathophysiology of tumours [16–18], comprehensive analysis of both miRNA and protein profiles within exosomes has not been conducted in haematopoietic tumours.

Lymphoma is a haematopoietic malignancy originating from lymphoid cells, and it is categorised into more than 80 distinct subtypes [19]. Among them, Non-Hodgkin lymphoma (NHL) is the most common type of lymphoma. Nevertheless, miRNA or protein profile within exosomes has not been examined in NHL.

In recent years, naturally occurring canine tumours were regarded as potential models of human tumours. In particular, canine lymphoma shares many characteristics of human NHL, including clinical presentation, immunophenotypic composition, chemotherapeutic protocols, and response to treatment [20,21]. Therefore, canine lymphoma has been advocated as an ideal model for studying human NHL.

Based on these backgrounds, we considered that comprehensive analyses of both miRNA and protein profiles within exosomes derived from canine lymphoid tumour cell lines could provide useful insights for understanding the molecular profiles and biological functions of exosomes derived from human lymphoid tumours. The aim of this study was to comprehensively analyse the miRNA and protein profiles within the exosomes released from canine lymphoid tumour cells.

Results

Exosome isolation and preparation of total RNA of exosomes and parent cells

The size distributions of exosomes isolated from four canine lymphoid tumour cell lines, CLBL-1, GL-1, UL-1, and Ema, are shown in [S1 Fig](#). The average size was between approximately 100–150 nm in each cell line. The RNA integrity numbers (RINs) and size distributions of total RNA samples taken from exosomes and parent cells are shown in [S2 Fig](#). Although there were common peaks corresponding to ribosomal RNAs in exosomal RNA of the four cell lines, the distributions of RNA sizes were clearly different between exosomes and parent cells.

Exosomal miRNA profiles

At first, the miRNA profiles of exosomes and parent cells were investigated via small RNA sequencing analysis. A minimum of 20 million raw reads were generated for each sample (see [S1 Table](#)).

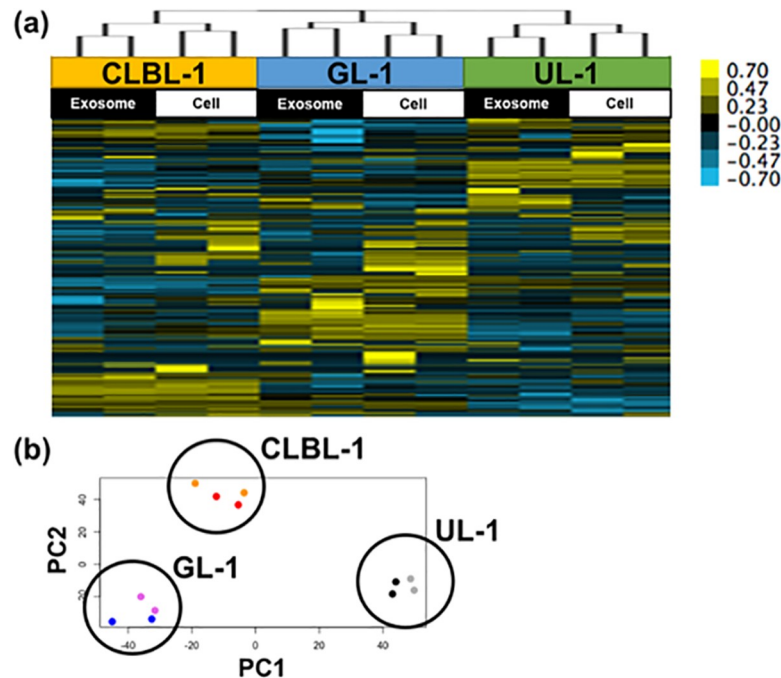


Fig 1. Hierarchical clustering (a) and PCA plots (b) for miRNA profiles of exosomes and parent cells of CLBL-1, GL-1, and UL-1. Exosomes and parent cells clustered similarly for each cell line and the profiles were different among cell lines. Orange dots (exosomes) and red dots (parent cells) correspond to CLBL-1, violet dots (exosomes) and blue dots (parent cells) to GL-1, and grey dots (exosomes) and black dots (parent cells) to UL-1.

<https://doi.org/10.1371/journal.pone.0208567.g001>

The number of reads mapped to miRNA and the mapping rate to miRNA was comparatively lower in Ema than the other three cell lines. Therefore, data for Ema were omitted in the statistical comparison of the quantities of miRNAs among cell lines using small RNA sequencing data.

Then, hierarchical clustering using the amounts of miRNA in CLBL-1, GL-1, and UL-1 was conducted. This analysis yielded three clusters composed of exosomes and parent cells of each cell line (Fig 1A). In addition, in the PCA plots, exosomes and cells clustered similarly for each cell line (Fig 1B). The results of these analyses were similar when the data from Ema were included (see S3 Fig).

The top ten miRNAs contained in exosomes and parent cells are listed in Table 1. Among these miRNAs, five miRNAs (let-7f, let-7g, miR-7, miR-30d, and miR-92a) were commonly contained in exosomes and cells of the four cell lines.

In the comparison of the amounts of miRNAs between cells and exosomes, the amounts of 39, 20, and 24 miRNAs were significantly different in CLBL-1, UL-1, and Ema, respectively ($q < 0.01$) (Fig 2). Among these miRNAs, the amount of miR-350 was significantly higher in exosomes than parent cells in all the three cell lines, and those of miR-22, miR-671, and miR-8865 were significantly lower in exosomes than parent cells in these cell lines (see S4 Fig). On the other hand, no miRNA displayed a significant difference in amount between exosomes and cells in GL-1.

The difference in the amount of miR-350 between exosomes and parent cells was confirmed by RT-qPCR (Fig 3). However, the amounts of miR-22, miR-671, and miR-8865 were not significantly different between exosomes and parent cells according to RT-qPCR. Following quantitative analysis, prediction of target genes was conducted for miR-350 using miRbase, and the top 10 target genes of the miRNA were extracted (see S2 Table). These target genes of

Table 1. The top 10 miRNAs abundantly contained in the exosomes and parent cells.

CLBL-1		GL-1		UL-1		Ema	
Exosome	Parent cell	Exosome	Parent cell	Exosome	Parent cell	Exosome	Parent cell
miR-148a	miR-148a	miR-148a	miR-148a	miR-7	miR-7	miR-7	let-7g
miR-7	let-7g	let-7f	let-7g	miR-378	miR-99a	let-7g	miR-7
let-7g	miR-363	let-7g	miR-10a	miR-99a	miR-378	let-7f	miR-363
let-7f	miR-7	miR-30d	let-7f	miR-30d	miR-30d	miR-30d	let-7f
miR-146a	miR-99a	miR-10a	miR-30d	let-7g	let-7g	miR-363	miR-30d
miR-30d	miR-30d	miR-378	miR-378	let-7f	miR-10a	miR-21	miR-21
miR-99a	miR-128	miR-7	miR-7	miR-363	miR-363	miR-148a	miR-128
miR-20a	miR-92a	let-7a	miR-128	miR-10a	miR-128	miR-26a	miR-26a
miR-378	let-7f	miR-103	miR-21	miR-92a	let-7f	miR-155	miR-92a
miR-92a	miR-146a	miR-92a	let-7a	miR-103	miR-25	miR-92a	miR-155

<https://doi.org/10.1371/journal.pone.0208567.t001>

miR-350 did not include those previously reported to be associated with the pathophysiology of tumour cells.

Exosomal protein profiles

The results of separating exosomal proteins from each cell line by SDS-PAGE are shown in S5 Fig. Exosomal protein profiles were investigated by liquid chromatography-tandem mass spectrometry (LC-MS/MS). This analysis identified a total of 1,890 proteins based on the sequences of the peptides extracted from exosomes of the four cell lines.

The top twenty proteins that were detected in each cell line by LC-MS/MS are listed in Table 2. As is the case with miRNAs, 13 proteins were commonly contained in the four cell lines. The abundantly contained proteins included those related to the cytoskeleton (β-actin

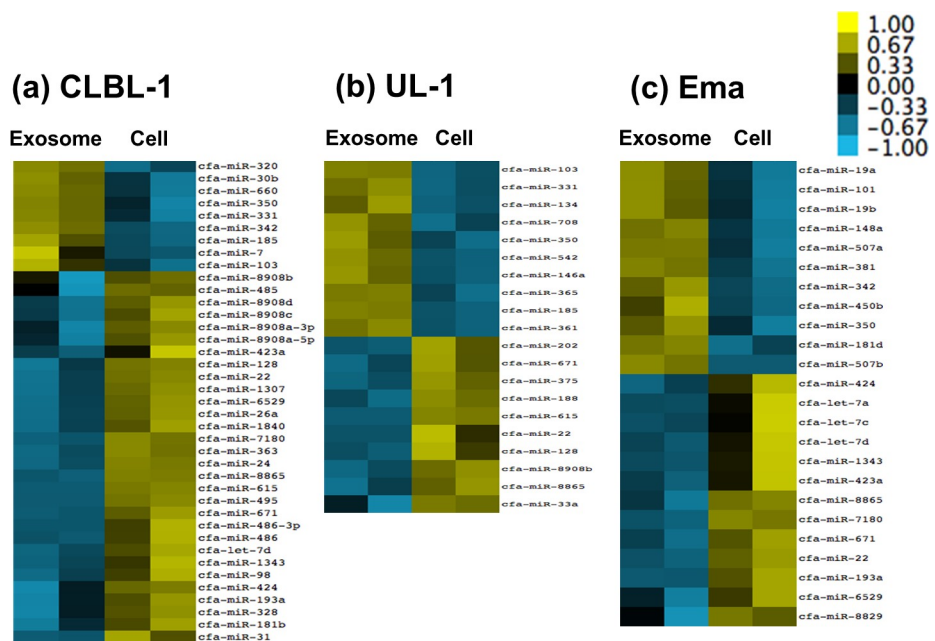


Fig 2. Heat maps showing miRNAs whose amounts were significantly different between exosomes and parent cells. The amounts of 39, 20, and 24 miRNAs were significantly different in CLBL-1 (a), UL-1 (b), and Ema (c), respectively ($q < 0.01$).

<https://doi.org/10.1371/journal.pone.0208567.g002>

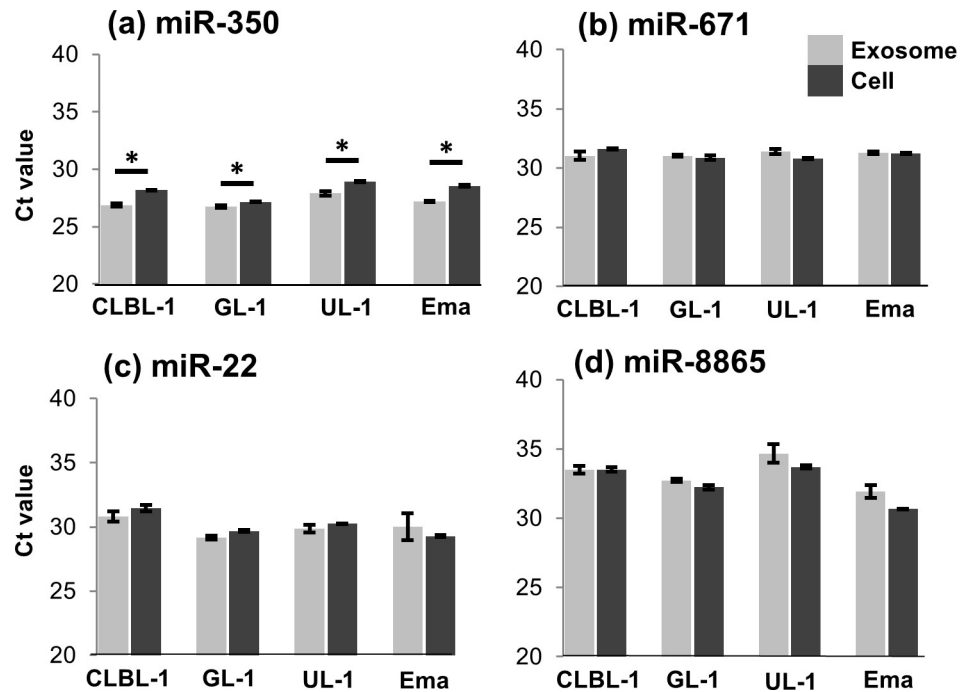


Fig 3. Comparison of the amounts of miR-350, miR-671, miR-22, and miR-8865 between exosomes and parent cells. The amount of miR-350 (a) is significantly higher in exosomes compared with parent cells, whereas those of miR-22 (c), miR-671 (b), and miR-8865 (d) were not significantly different. All data represent the mean \pm SD of three independent experiments. * $P < 0.05$.

<https://doi.org/10.1371/journal.pone.0208567.g003>

and tubulins) and heat shock proteins. Except for these abundant proteins, CD63 was detected in exosomes of all four cell lines and CD81 was detected in those of CLBL-1, GL-1 and UL-1 among the exosome marker proteins, although CD9 was not detected in any cell lines.

Comparison of exosomal miRNA and protein profiles between vincristine sensitive (VCR-S) cell lines and vincristine resistant (VCR-R) cell lines

The exosomal miRNA profiles were also compared between the VCR-S cell lines (CLBL-1 and GL-1) and the VCR-R cell line (UL-1) (see [S6 Fig](#)). In data from small RNA sequencing, the amounts of 11 miRNAs within exosomes were significantly lower in VCR-S cell lines than the VCR-R cell line, and those of 5 miRNAs were significantly higher in VCR-S cell lines than the VCR-R cell line ($q < 0.01$). In parent cells, the amounts of 8 miRNAs were significantly lower in VCR-S cell lines than the VCR-R cell line, and those of 7 miRNAs were higher in VCR-S cell lines than the VCR-R cell line ($q < 0.01$).

Among these miRNAs, the significant differences in the amounts of miR-151, miR-8908a-3p, and miR-486 were confirmed by RT-qPCR using the four cell lines including Ema, which is resistant to VCR ([Fig 4](#)). The amounts of miR-151 and miR-8908a-3p within exosomes and parent cells in VCR-S cell lines were significantly lower than VCR-R cell lines ($P < 0.01$). The amount of miR-486 within exosomes and parent cells in VCR-S cell lines was significantly higher than VCR-R cell lines ($P < 0.01$). The target genes were predicted for miR-151, miR-8908a-3p, and miR-486, and the top 10 target genes of each miRNA were extracted (see [S2 Table](#)). These genes included those that have been reported to be associated with the biological behaviour of tumour cells (*NTRK2*, *MAPK8*, *BCOR*, and *PIK3R1* genes).

Table 2. The top 20 proteins abundantly contained in exosomes.

CLBL-1	GL-1	UL-1	Ema
ACTB	ACTB	ACTB	ACTB
TUBB	TUBB	TUBB	TUBB
TUBB4B	TUBB4B	TUBB4B	TUBB4B
TUBB2B	TUBB2B	TUBB2B	TUBB2B
TUBB4A	TUBB4A	TUBB4A	TUBB4A
TUBA1C	TUBA1C	TUBA1C	TUBA1C
TUBA4A isoform X1	TUBA4A isoform X1	TUBA4A isoform X1	TUBA4A isoform X1
FLNA	FLNA	FLNA	FLNA
TLN1 isoform X4	TLN1 isoform X4	TLN1 isoform X4	TLN1 isoform X4
MYH9	MYH9	MYH9	MYH9
FAS	FAS	FAS	FAS
EEF2	EEF2	EEF2	EEF2
ACLY isoform X1	ACLY isoform X1	ACLY isoform X1	ACLY isoform X1
HSP90B	NCL	HSP90B	HSP90B
CCT2 isoform X1	IQGAP1	CCT2 isoform X1	CCT2 isoform X1
TUBBA3	DYNC1H1	DYNC1H1	DYNC1H1
CCT8 isoform X2	CLTC isoform X1	CLTC isoform X1	CLTC isoform X1
CCT8 isoform X1	GAPDH	GAPDH	GAPDH
CENP	CENP	EEF1A1	EEF1A1
HSP71	HSP71	EPRS isoform X1	PKM isoform X1

<https://doi.org/10.1371/journal.pone.0208567.t002>

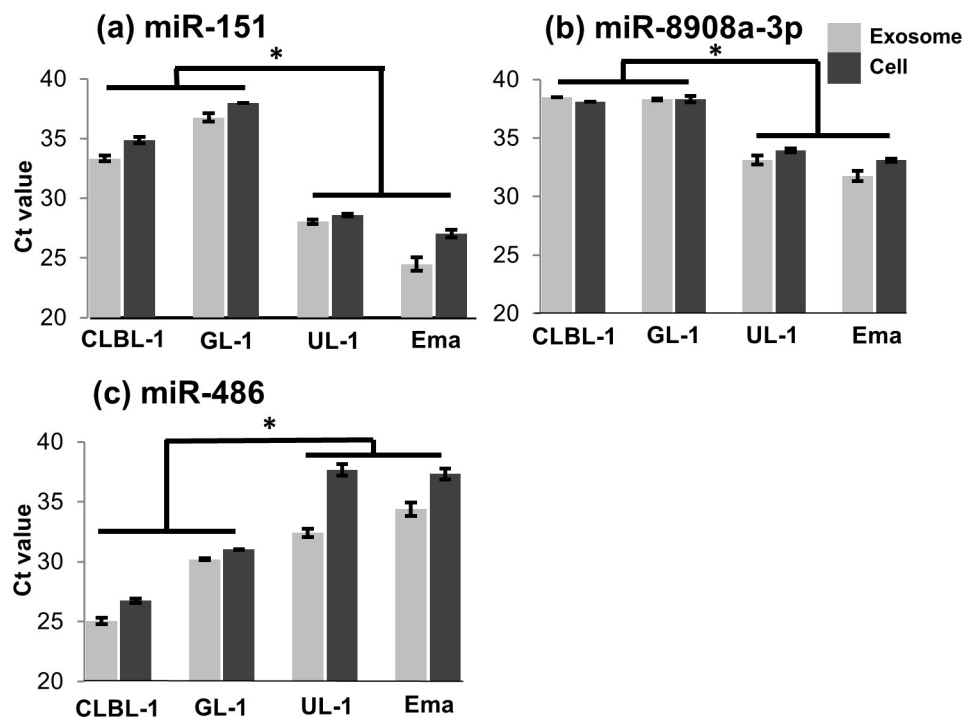


Fig 4. Comparison of the amounts of miR-151, miR-8908a-3p, and miR-486 between VCR-S and VCR-R cell lines. The amounts of miR-151 (a) and miR-8908a-3p (b) in VCR-S cell lines were significantly lower than in VCR-R cell lines, and that of miR-486 (c) in VCR-S cell lines were significantly higher than in VCR-R cell lines. All data represent the mean \pm SD of three independent experiments. *P < 0.05.

<https://doi.org/10.1371/journal.pone.0208567.g004>

Table 3. Exosomal proteins detected only in vincristine-sensitive or vincristine-resistant cell lines.

Protein name	Total spectral count			
	CLBL-1	GL-1	UL-1	Ema
CD82	13	14	-	-
CD20 isoform X1	59	-	-	-
HLA-DRA	47	-	-	-
MHC class II beta	44	-	-	-
HLA-DQB	22	-	-	-
MHC class II	13	-	-	-
CD74 isoform X2	7	-	-	-
HLA-DQA	30	-	-	-
IGH constant region CH2	31	-	-	-
IGJ isoform X1	14	-	-	-
GZMK	-	-	23	59
PLOD1	-	-	14	36
HUWEI isoform X2	-	-	6	36
KLC1 isoform X8	-	-	8	14
HK2	-	-	60	13
DHX29	-	-	7	13
GANAB isoform X1	-	-	6	12
PWP1	-	-	5	10
EIF2B2	-	-	7	10
THOC2 isoform X1	-	-	8	9

-, not detected

<https://doi.org/10.1371/journal.pone.0208567.t003>

Following the LC-MS/MS analysis, proteins that were detected only in VCR-S or VCR-R cell lines were also extracted (Table 3). Among these proteins, the difference in the amount of CD82 was validated by western blotting (Fig 5). CD82 was detected in exosomes of CLBL-1 and GL-1, while no band corresponding to CD82 was detected in exosomes of UL-1 and Ema. This protein was not detected in parent cells of all the four cell lines. HSP90B, which was selected as a protein that is abundantly contained in exosomes, was detected in exosomes from all four of the cell lines.

Discussion

In the present study, the miRNA and protein profiles within exosomes derived from four canine lymphoid tumour cell lines were comprehensively analysed by small RNA sequencing and LC-MS/MS. The novel findings of this study are summarised in Table 4.

In small RNA sequencing, the number of reads mapped to miRNA and the mapping rate to miRNA were comparatively lower in both exosomes and parent cells of Ema than the other three cell lines. These results suggested that the total amount and proportions of miRNAs in total RNA within exosomes or parent cells were lower in Ema than the other 3 cell lines, since the same amount of RNA of Ema was used as the other 3 cell lines. In the hierarchical clustering analysis and PCA plots for three cell lines, three distinct clusters composed of the exosomes and parent cells of each cell line were observed, and the results of these analyses were similar when the data from Ema were included. Therefore, it was indicated that the miRNA profiles differed among the exosomes of each cell line, which corresponded to the expression patterns of the parent cells.

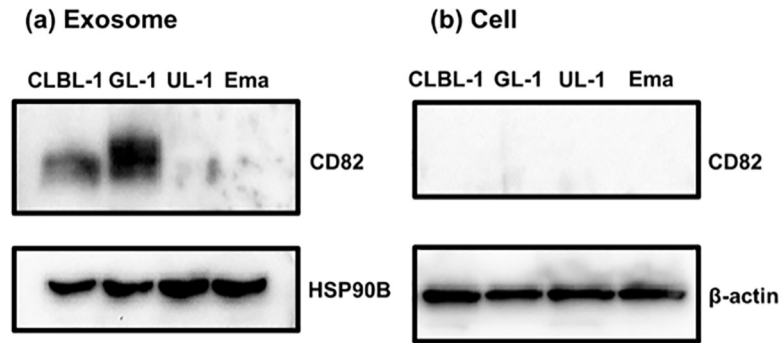


Fig 5. Western blotting for CD82 using proteins extracted from exosomes (a) and parent cells (b) of each cell line. HSP90B and β -actin were selected for internal control for exosomes and parent cells, respectively. CD82 protein is detected in the exosomes of CLBL-1 and GL-1, whereas it was not detected in parent cells in any of the four cell lines. The figures that shows the detection of CD82 within exosomes and parent cells were cropped from the different parts of the same figure of the membrane. The figures of HSP90B and β -actin were cropped from the figures of the different membrane. The full-length figures of blotting membrane are shown in *S7 Fig*.

<https://doi.org/10.1371/journal.pone.0208567.g005>

Small RNA sequencing also revealed that five major miRNAs (let-7f, let-7g, miR-7, miR-30d, and miR-92a) extracted from exosomes or parent cells were similar among the four cell lines. Previous studies have reported that exosomes derived from tumour cells contain miRNAs of the let-7 family [22,23]. It has also been reported that miR-30d and miR-92a are abundant in exosomes of Gamma-Herpesvirus-infected lymphoma cell lines [12]. Therefore, these miRNAs might be associated with the pathophysiology of lymphoid tumours.

In the comparison of the amounts of miRNAs between exosomes and parent cells, significant differences were observed for 39, 20, and 24 miRNAs in CLBL-1, UL-1, and Ema, respectively, whereas there was no significant difference in GL-1. Among these miRNAs, the significant differences in the amounts of miR-350 between exosomes and parent cells were confirmed in all four cell lines by RT-qPCR, which is one of the novel findings of the present study. These results suggested that miR-350 might be a molecule selectively incorporated into exosomes in lymphoid tumour cells. The predicted target genes of miR-350 did not include those previously reported to be associated with the pathophysiology of tumour cells. However, miR-350 was reported to promote apoptosis through down-regulation of *PIK3R3* gene [24]. Considering the previous reports that lymphoma cells inactivate natural killer cells and suppress anti-tumour immune response [7–9], exosomal miR-350 released from lymphoid tumour cells might be associated with inactivation of the immune cells in the tumor microenvironments.

LC-MS/MS analysis revealed that exosomes derived from each cell line contain various types of protein. Most of the proteins abundantly contained in exosomes were common

Table 4. Summary of the novel findings of this study.

		VCR-S cell lines				VCR-R cell lines			
		CLBL-1		GL-1		UL-1		Ema	
		Exosome	Cell	Exosome	Cell	Exosome	Cell	Exosome	Cell
miRNAs	miR-350	High	Low	High	Low	High	Low	High	Low
	miR-151	Low				High			
	miR-8908a-3p	Low				High			
	miR-486	High				Low			
Protein	CD82	Detected	N.D.	Detected	N.D.	N.D.	N.D.	N.D.	N.D.

N.D., Not detected

<https://doi.org/10.1371/journal.pone.0208567.t004>

among the four cell lines, including those related to cytoskeleton, such as β -actin, tubulins, and heat shock proteins. In addition, CD63 or CD81 were also detected in exosomes derived from each cell line. Exosomal markers have been reported to include members of the tetraspanin family (CD9, CD63, and CD81) and heat shock proteins (HSP60, HSP70, and HSP90) [25,26]. It was also reported that exosomes derived from Jurkat cells contain β -actin and tubulins [27]. Thus, those results in previous studies are consistent with those in the present study.

In the comparison of the amounts of miRNA within the exosomes, the amounts of miR-151, miR-8908a-3p, and miR-486 were confirmed to be different between VCR-S cell lines and VCR-R cell lines by RT-qPCR. The amounts of miR-151 and miR-8908a-3p were significantly lower in VCR-S cell lines, while miR-486 was significantly more abundant in these cell lines. In a previous report of the comparison of exosomal miRNA profiles between drug sensitive and resistant lymphoma cells, the expression levels of miR-99a-5p and miR-125b-5p were significantly higher in chemotherapy resistant patients than in chemotherapy sensitive patients [28]. However, there have been no studies on the differences of the amounts of exosomal or cellular miR-151, miR-8908a-3p, and miR-486 between chemotherapy-sensitive and -resistant lymphoid tumours. The target genes of miR-151 included the gene *NTRK2*, a member of neurotrophic tyrosine receptor kinase family. The expression of *NTRK2* was reported to be down-regulated in patients with breast cancer with a poor prognosis [29]. The expression of this gene was also reported to suppress anoikis by activating the PI3K/Akt pathway in human ovarian cancer cells [30]. The target genes of miR-8908a-3p included *MAPK8* (also known as *JNK1*) and *BCOR*. The *MAPK8* gene is a member of the MAP kinase and JNK family, and involved in various cellular processes including cell proliferation, differentiation, and apoptosis [31,32]. The *BCOR* gene encodes a co-repressor of BCL6, a transcriptional repressor that is required for formation of germinal centres [33,34] and silences various genes involved in the cell cycle and apoptosis [35]. The target genes of miR-486 included *PIK3R1*, one of the oncogenes that promotes cell proliferation and tumour cell invasion [36]. Based on these evidences, it is possible that these miRNAs might be associated with the drug resistance in lymphoid tumours via modification of target gene expressions in parent tumour cells. In our previous report, in addition, expression of genes related to immune responses and inflammatory reactions was decreased in tumour tissues obtained from canine lymphoma patients at chemotherapy resistant phases [37]. Therefore, it is also possible that these miRNAs within exosomes might cause inactivation of immune response and inflammatory reaction in lymphoid tumour tissues.

Among the proteins detected by LC-MS/MS in the present study, CD82 was detected in the exosomes of VCR-S cell lines but not in those of VCR-R cell lines, and the difference in its amount was confirmed by western-blotting. In addition, CD82 was not detected in proteins extracted from parent cells of CLBL-1 and GL-1, suggesting that CD82 was selectively delivered into exosomes in these cell lines. Since expression of CD82 within exosomes has not been reported in lymphoid tumours, this is a newly identified exosomal protein that might be associated with drug resistance in these tumours. CD82 has been reported to suppress tumour metastasis [38] and be associated with tumour cell growth [39] and survival [40]. In breast cancer, CD82 was also reported to redistribute from tumour tissues to exosomes [41]. It is possible that decreased amounts of CD82 within exosomes might be due to redistribution from tumour tissues and it might be associated with drug resistance through promotion of metastasis and tumour cell survival in lymphoid tumours.

In conclusion, most of the miRNAs and proteins abundantly contained in exosomes are common among the four cell lines, but the miRNA profiles in exosomes reflect those of parent cells and differ among cell lines. In addition, miR-151, miR-8908a-3p, miR-486, and CD82 proteins were differentially abundant within the exosomes between VCR-S and VCR-R cell

lines. Further investigations are needed to elucidate the biological functions of these molecules in the crosstalk between tumour cells and tumour microenvironment.

Materials and methods

Cell lines and cell culture

Four canine lymphoid tumour cell lines (CLBL-1, GL-1, UL-1, and Ema) were used in this study: CLBL-1, a canine B-cell lymphoma cell line [42]; GL-1, a canine B-cell leukaemia cell line [43]; UL-1, a canine T-cell lymphoma cell line [44]; and Ema; a canine T-cell lymphoma cell line [45]. UL-1 and Ema were established from dogs with lymphoma showing drug resistance after chemotherapy, whereas CLBL-1 and GL-1 were established from dogs with leukaemia or lymphoma who were not subjected to chemotherapy. CLBL-1, GL-1, and Ema were kindly provided by Dr. Rütgen, University of Veterinary Medicine Vienna, Austria, Dr. Nakai-chi, Yamaguchi University, Japan, and Dr. Mizuno, Yamaguchi University, Japan, respectively. Our group established UL-1 previously [44]. Our previous study reported that CLBL-1 and GL-1 were sensitive to vincristine, and UL-1 and Ema were resistant to vincristine [46]. These cell lines were cultured in RPMI-1640 medium at 37°C, with 10% foetal bovine serum (Biowest, Nuaille, France) in a humidified atmosphere containing 5% CO₂.

Exosome isolation and preparation of total RNA and protein of exosomes and parent cells

Exosomes were isolated from 3×10⁷ cells (CLBL-1, GL-1, and UL-1) and 2×10⁷ cells (Ema) cultured for 24h in growth medium without foetal bovine serum. We used reduced number of Ema cells because they proliferate faster than other cell lines and become confluent during cultivation if 3×10⁷ cells were used at the start of the cultivation for exosome isolation. Exosomes were isolated from cell culture media using the Total Exosome Isolation (from cell culture media) (ThermoFisher Scientific, Waltham, MA, USA), and exosome protein and RNA were prepared using the Total Exosome RNA and Protein Isolation Kit (ThermoFisher Scientific) according to the manufacturer's instructions. The number and sizes of isolated exosomes were measured using NanoSight NS300 system (Malvern Instruments, Malvern, UK). The concentrations of exosome protein samples were measured using Micro BCA Protein Assay (ThermoFisher Scientific), and the concentrations and size distributions of exosomal RNA samples were measured using Agilent RNA 6000 Pico Kit and Agilent 2100 Bioanalyzer (Agilent Technologies, Palo Alto, CA, USA). Total RNA of each parent cell line was extracted using miR-Neasy Mini Kit (QIAGEN, Limburg, Netherlands), and concentration and integrity were measured as described above. Each total RNA sample was prepared in duplicate.

Small RNA sequencing and data processing

Small RNA sequencing libraries were prepared with 156 ng of total RNA using NEB Next Multiplex Small RNA Library Prep Kit (New England Biolabs, Ipswich, MA, USA). RNA sequencing was performed in duplicate using NextSeq500 (Illumina, San Diego, CA, USA) with High Output Kit (Illumina) as stranded, single 36-base reads following the manufacturer's instruction.

Raw BCL data for each sample were de-multiplexed with bcl2fastq (version 2.18.0.12) and were stored in independent FASTQ files. The sequence data were trimmed with Trimomatic (version 0.36) [47] to clean up sequences with low-quality and those with sequencing adaptors. After trimming, a subset of short reads was aligned to cfa_MiR_453 (<http://www.targetscan.org/>) with Bowtie2 (version 2.2.9) [48]. The depth of the reads aligned to cfa_MiR_453 was

quantified using Samtools (version 1.3.1). Counts per million (CPM) was imported into R (version 3.3.2) and principal component analysis was conducted. Then, miRNA counts for each sample were imported into R for differential expression analysis with EdgeR [49,50]. Cluster3.0 and Java Treeview (version 1.1.6r4) were used for hierarchical clustering and visualization. The data from small RNA sequencing in this study are available in the DDBJ Sequenced Read Archive database with the accession number DRA006696 (<https://ddbj.nig.ac.jp/DRAsearch/submission?acc=DRA006696>).

Quantitative real-time RT-PCR

The amounts of miRNAs extracted from the small RNA sequencing data were validated by RT-qPCR using TaqMan MicroRNA Assay (Applied Biosystems, Foster City, CA, USA). The candidate miRNAs selected for validation are listed in the [S3 Table](#) online. Briefly, 3.3 ng of total RNA was reverse transcribed using TaqMan MicroRNA Reverse Transcription Kit (Applied Biosystems), and qPCR was performed using TaqMan MicroRNA Assay and Thermal Cycler Dice Real Time System TP800 (Takara Bio, Shiga, Japan). Data were expressed as mean C_T values of three independent experiments performed in triplicate. C_T values were determined using the second derivative maximum method, in which a C_T value is expressed as the cycle number at which the second derivative was at its maximum. After validation, target genes of the miRNAs were predicted using miRbase (<http://www.mirbase.org/>) [51,52].

LC-MS/MS

Protein profiles of exosomes were analysed by LC-MS/MS. An EASY-Spray column (15 cm \times 75 μ m I.D., 3 μ m, ThermoFisher Scientific) was employed for separation of each exosomal protein sample at the flow rate of 300 nl/min. The amount of exosomal protein used was 2 μ g. A quadrupole tandem mass spectrometer (Q Exactive Plus, ThermoFisher Scientific) was used in positive ion mode for analytic detection. The raw MS spectra data were queried against the NCBI Canine protein sequence database using the MASCOT database search engine, and peptides were quantified according to the spectral counts.

Western-blotting

Expressions of the candidate proteins extracted from the LC-MS/MS data were verified by western blotting. One μ g of protein extracted from exosome or parent cells was separated by SDS-PAGE and blotted onto a PVDF membrane. The membranes were blocked in 5% skimmed milk and incubated with primary antibodies against CD82, HSP90B, or β -actin. HSP90B was selected as the internal control of the exosomal protein. Then, the membranes were incubated with secondary antibodies. The antibodies, dilutions, and incubation temperatures are shown in the [S4 Table](#) online. After incubation, positive immunoreactivity was detected using Luminata Forte Western HRP Substrate (Merck Millipore, Darmstadt, Germany) and visualized using a ChemiDoc XRS Plus (Bio-Rad Laboratories, Hercules, CA, USA).

Statistical analysis

In the differential expression analysis using EdgeR, a false discovery rate (q-value) of less than 0.01 was considered statistically significant. One-way ANOVA followed by Tukey's post-hoc test was performed for multiple comparisons of miRNA quantities in the RT-qPCR using the STATMATE (ATMS, Tokyo, Japan) software, and P-values of less than 0.05 were considered statistically significant.

Supporting information

S1 Table. Mean numbers of raw reads, reads mapped to miRNA, and mapping rates to miRNA.

(XLSX)

S2 Table. Top 10 predicted target genes of miRNAs extracted in the present study.

(XLSX)

S3 Table. miRNAs selected for validation by RT-qPCR and TaqMan MicroRNA Assay IDs for these miRNAs.

(XLSX)

S4 Table. Primary and secondary antibodies for detection of CD82, HSP90B, and β -actin.

(XLSX)

S1 Fig. Size distributions of exosomes of CLBL-1 (a), GL-1 (b), UL-1 (c), and Ema (d).

(TIF)

S2 Fig. RINs and size distributions of total RNA samples from exosomes and parent cells.

“18S” indicates the peak corresponds to 18S ribosomal RNA, and “28S” indicates that corresponds to 28S ribosomal RNA.

(TIF)

S3 Fig. PCA plots analysis including data of Ema cell line. Exosomes and parent cells clustered similarly for each cell line and the profiles are different among cell lines. Orange dots (exosomes) and red dots (parent cells) correspond to CLBL-1, violet dots (exosomes) and blue dots (parent cells) to GL-1, grey dots (exosomes) and black dots (parent cells) to UL-1, and yellow dots (exosomes) and green dots (parent cells) to Ema.

(TIF)

S4 Fig. Venn diagram showing common miRNAs with significant differences in amounts between exosomes and parent cells. The names of miRNAs whose amounts were significantly larger in exosomes than parent cells are shown in red, and those whose amounts were significantly smaller in exosomes than parent cells are shown in blue.

(TIF)

S5 Fig. Separation of exosomal proteins of each cell line by SDS-PAGE. Lane M is the protein ladder. Lanes 1–4 correspond to the exosomal proteins extracted from CLBL-1, GL-1, UL-1, and Ema, respectively, and lanes 1’-4’ correspond to exosomal proteins precipitated with trichloroacetic acid extracted from CLBL-1, GL-1, UL-1, and Ema, respectively.

(TIF)

S6 Fig. Heat maps showing the miRNAs whose amounts were significantly different between VCR-S and VCR-R cell lines. In exosomes (a), the amounts of 11 miRNAs were significantly lower in VCR-S cell lines than VCR-R cell line, and those of 5 miRNAs were significantly higher in VCR-S cell lines than VCR-R cell line. In parent cells (b), the amounts of 8 miRNAs were significantly lower in VCR-S cell lines than VCR-R cell line, and those of 7 miRNAs were higher in VCR-S cell lines than VCR-R cell line.

(TIF)

S7 Fig. Figures of full length blotting membrane used for detection of CD82, HSP90B, and β -actin. The figures of the same membrane were shown in (a) and (b), but exposure times were different between these figures. In Fig 5, the figures that show the detection of CD82 within exosomes and parent cells were cropped from the different parts of (b). The figures of

detection of HSP90B and β -actin were cropped from (c) and (d), respectively. (TIF)

Author Contributions

Conceptualization: Hirotaka Tomiyasu, Yuko Goto-Koshino, Koichi Ohno, Hajime Tsujimoto.

Formal analysis: Hirotaka Tomiyasu.

Funding acquisition: Hirotaka Tomiyasu.

Investigation: Hajime Asada, Takao Uchikai.

Project administration: Hirotaka Tomiyasu.

Resources: Hajime Asada.

Supervision: Hirotaka Tomiyasu.

Validation: Hajime Asada.

Visualization: Hajime Asada.

Writing – original draft: Hajime Asada, Hirotaka Tomiyasu, Takao Uchikai.

Writing – review & editing: Hirotaka Tomiyasu, Takao Uchikai, Genki Ishihara, Yuko Goto-Koshino, Koichi Ohno, Hajime Tsujimoto.

References

1. Zoller M. Janus-faced myeloid-derived suppressor cell exosomes for the good and the bad in cancer and autoimmune disease. *Front Immunol.* 2011; 9: 137.
2. Bebelman MP, Smit MJ, Pegtel DM, Baglio SR. Biogenesis and function of extracellular vesicles in cancer. *Pharmacol Ther.* 2018 S0163-7258(18)30038-X.
3. Dai G, Yao X, Zhang Y, Gu J, Geng Y, Xue F, et al. Colorectal cancer cell-derived exosomes containing miR-10b regulate fibroblast cells via the PI3K/Akt pathway. *Bull Cancer.* 2018; 105: 336–349. <https://doi.org/10.1016/j.bulcan.2017.12.009> PMID: 29496262
4. Piao YJ, Kim HS, Hwang EH, Woo J, Zhang M, Moon WK. Breast cancer cell-derived exosomes and macrophage polarization are associated with lymph node metastasis. *Oncotarget.* 2018; 9: 7398–7410. <https://doi.org/10.18632/oncotarget.23238> PMID: 29484119
5. Bardi GT, Smith MA, Hood JL. Melanoma exosomes promote mixed M1 and M2 macrophage polarization. *Cytokine.* 2018; 105: 63–72. <https://doi.org/10.1016/j.cyto.2018.02.002> PMID: 29459345
6. An M, Zhu J, Wu J, Cuneo KC, Lubman DM. Circulating exosomes from pancreatic cancer accelerate the migration and proliferation of PANC-1 cells. *J Proteome Res.* 2018; 17: 1690–1699. <https://doi.org/10.1021/acs.jproteome.8b00014> PMID: 29494150
7. Yang YZ, Zhang XY, Fang LJ, Wan Q, Li J. Role of exosomes in the cross-talk between leukemia cells and mesenchymal stem cells -Review. *Zhongguo Shi Yan Xue Ye Xue Za Zhi.* 2017; 25: 1255–1258. <https://doi.org/10.7534/j.issn.1009-2137.2017.04.053> PMID: 28823304
8. Xu B, Wang T. Intimate cross-talk between cancer cells and the tumor microenvironment of B-cell lymphomas: The key role of exosomes. *Tumour Biol.* 2017; 39: 1010428317706227. <https://doi.org/10.1177/1010428317706227> PMID: 28618932
9. Hedlund M, Nagaeva O, Kargl D, Baranov V, Mincheva-Nilsson L. Thermal- and oxidative stress causes enhanced release of NKG2D ligand-bearing immunosuppressive exosomes in leukemia/lymphoma T and B cells. *PLoS One.* 2011; 6: e16899. <https://doi.org/10.1371/journal.pone.0016899> PMID: 21364924
10. Min QH, Wang XZ, Zhang J, Chen QG, Li SQ, Liu XQ, et al. Exosomes derived from imatinib-resistant chronic myeloid leukemia cells mediate a horizontal transfer of drug-resistant trait by delivering miR-365. *Exp Cell Res.* 2018; 362: 386–393. <https://doi.org/10.1016/j.yexcr.2017.12.001> PMID: 29223442
11. Wang J, Li D, Zhuang Y, Fu J, Li X, Shi Q, et al. Exosomes derived from bone marrow stromal cells decrease the sensitivity of leukemic cells to etoposide. *Oncol Lett.* 2017; 14: 3082–3088. <https://doi.org/10.3892/ol.2017.6509> PMID: 28928845

12. Hoshina S, Sekizuka T, Kataoka M, Hasegawa H, Hamada H, Kuroda M, et al. Profile of exosomal and intracellular microRNA in gamma-herpesvirus-infected lymphoma cell lines. *PLoS One*. 2016; 11: e0162574. <https://doi.org/10.1371/journal.pone.0162574> PMID: 27611973
13. Nanbo A, Katano H, Kataoka M, Hoshina S, Sekizuka T, Kuroda M, et al. Infection of Epstein-Barr Virus in type III latency modulates biogenesis of exosomes and the expression profile of exosomal miRNAs in the burkitt lymphoma mutu cell lines. *Cancers*. 2018; 10: pii: E237.
14. Yeh YY, Ozer HG, Lehman AM, Maddocks K, Yu L, Johnson AJ, et al. Characterization of CLL exosomes reveals a distinct microRNA signature and enhanced secretion by activation of BCR signaling. *Blood*. 2015; 125: 3297–3305. <https://doi.org/10.1182/blood-2014-12-618470> PMID: 25833959
15. Prieto D, Sotelo N, Seija N, Sernbo S, Abreu C, Duran R, et al. S100-A9 protein in exosomes from chronic lymphocytic leukemia cells promotes NF- κ B activity during disease progression. *Blood*. 2017; 130: 777–788. <https://doi.org/10.1182/blood-2017-02-769851> PMID: 28596424
16. Asadirad A, Hashemi SM, Baghaei K, Ghanbarian H, Mortaz E, Zali MR, et al. Phenotypical and functional evaluation of dendritic cells after exosomal delivery of miRNA-155. *Life Sci*. 2019; 219: 152–162. <https://doi.org/10.1016/j.lfs.2019.01.005> PMID: 30625290
17. Tang X, Lu H, Dooner M, Chapman S, Quesenberry PJ, Ramratnam B. Exosomal Tat protein activates latent HIV-1 in primary, resting CD4+ T lymphocytes. *JCI Insight*. 2018; 3: e95676.
18. Clayton A, Harris CL, Court J, Mason MD, Morgan BP. Antigen-presenting cell exosomes are protected from complement-mediated lysis by expression of CD55 and CD59. *Eur J Immunol*. 2003; 33: 522–531. <https://doi.org/10.1002/immu.200310028> PMID: 12645951
19. Tamaru JI. 2016 revision of the WHO classification of lymphoid neoplasms. *Rinsho ketsueki*. 2017; 58: 2188–2193. <https://doi.org/10.11406/rinketsu.58.2188> PMID: 28978864
20. Seelig DM, Avery AC, Ehrhart EJ, Linden MA. The comparative diagnostic features of canine and human lymphoma. *Vet Sci*. 2016; 3: pii: 11.
21. Villarnovo D, McCleary-Wheeler AL, Richards KL. Barking up the right tree: advancing our understanding and treatment of lymphoma with a spontaneous canine model. *Curr Opin Hematol*. 2017; 24: 359–366. <https://doi.org/10.1097/MOH.0000000000000357> PMID: 28426554
22. Ohshima K, Inoue K, Fujiwara A, Hatakeyama K, Kanto K, Watanabe Y, et al. Let-7 microRNA family is selectively secreted into the extracellular environment via exosomes in a metastatic gastric cancer cell line. *PLoS One*. 2010; 5: e13247. <https://doi.org/10.1371/journal.pone.0013247> PMID: 20949044
23. Liao J, Liu R, Yin L, Pu Y. Expression profiling of exosomal miRNAs derived from human esophageal cancer cells by Solexa high-throughput sequencing. *Int J Mol Sci*. 2014; 15: 15530–15551. <https://doi.org/10.3390/ijms150915530> PMID: 25184951
24. Sui J, Fu Y, Zhang Y, Ma S, Yin L, Pu Y, et al. Molecular mechanism for miR-350 in regulating of titanium dioxide nanoparticles in macrophage RAW264.7 cells. *Chem Biol Interact*. 2018; 280: 77–85. <https://doi.org/10.1016/j.cbi.2017.12.020> PMID: 29247641
25. Simpson RJ, Lim JW, Moritz RL, Mathivanan S. Exosomes: proteomic insights and diagnostic potential. *Expert Rev Proteomics*. 2009; 6: 267–283. <https://doi.org/10.1586/epr.09.17> PMID: 19489699
26. Yoshioka Y, Konishi Y, Kosaka N, Katsuda T, Kato T, Ochiya T. Comparative marker analysis of extracellular vesicles in different human cancer types. *J Extracell Vesicles*. 2013; 2: 20424.
27. Bosque A, Dietz L, Gallego-Lleyda A, Sanclemente M, Iturralde M, Naval J, et al. Comparative proteomics of exosomes secreted by tumoral Jurkat T cells and normal human T cell blasts unravels a potential tumorigenic role for valosin-containing protein. *Oncotarget*. 2016; 7: 29287–29305. <https://doi.org/10.18632/oncotarget.8678> PMID: 27086912
28. Feng Y, Zhong M, Zeng S, Wang L, Liu P, Xiao X, et al. Exosome-derived miRNAs as predictive biomarkers for diffuse large B-cell lymphoma chemotherapy resistance. *Epigenomics*. 2019; 11: 35–51.
29. Li Z, Peng L, Han S, Huang Z, Shi F, Cai Z, et al. Screening molecular markers in early breast cancer of the same pathological types but with different prognoses using Agilent gene chip. *Nan Fang Yi Ke Da Xue Xue Bao*. 2013; 33: 1483–1488. PMID: 24144752
30. Yu X, Liu L, Cai B, He Y, Wan X. Suppression of anoikis by the neurotrophic receptor TrkB in human ovarian cancer. *Cancer Sci*. 2008; 99: 543–552. <https://doi.org/10.1111/j.1349-7006.2007.00722.x> PMID: 18201274
31. Cantley LC. The phosphoinositide 3-kinase pathway. *Science*. 2002; 296: 1655–1657. <https://doi.org/10.1126/science.296.5573.1655> PMID: 12040186
32. Wada T, Penninger JM. Mitogen-activated protein kinases in apoptosis regulation. *Oncogene*. 2004; 23: 2838–2849. <https://doi.org/10.1038/sj.onc.1207556> PMID: 15077147
33. Ci W, Polo JM, Melnick A. B-cell lymphoma 6 and the molecular pathogenesis of diffuse large B-cell lymphoma. *Curr Opin Hematol*. 2008; 15: 381–390. <https://doi.org/10.1097/MOH.0b013e328302c7df> PMID: 18536578

34. Hatzl K, Jiang Y, Huang C, Garret-Bakelman F, Gearhart MD, Giannopoulou EG, et al. A hybrid mechanism of action for BCL6 in B cells defined by formation of functionally distinct complexes at enhancers and promoters. *Cell Rep.* 2013; 4: 578–588. <https://doi.org/10.1016/j.celrep.2013.06.016> PMID: [23911289](https://pubmed.ncbi.nlm.nih.gov/23911289/)
35. Cardenas MG, Oswald E, Yu W, Xue F, MacKerell AD Jr, Melnick AM. The expanding role of the BCL6 oncoprotein as a cancer therapeutic target. *Clin Cancer Res.* 2017; 23: 885–893. <https://doi.org/10.1158/1078-0432.CCR-16-2071> PMID: [27881582](https://pubmed.ncbi.nlm.nih.gov/27881582/)
36. He S, Zhang J, Zhang W, Chen F, Luo R. FOXA1 inhibits hepatocellular carcinoma progression by suppressing PIK3R1 expression in male patients. *J Exp Clin Cancer Res.* 2017; 36: 175. <https://doi.org/10.1186/s13046-017-0646-6> PMID: [29208003](https://pubmed.ncbi.nlm.nih.gov/29208003/)
37. Suenaga M, Tomiyasu H, Watanabe M, Ogawa K, Motegi T, Goto-Koshino Y, et al. Comprehensive analysis of gene expression profiles reveals novel candidates of chemotherapy resistant factors in canine lymphoma. *Vet J.* 2017; 228: 18–21. <https://doi.org/10.1016/j.tvjl.2017.10.002> PMID: [29153103](https://pubmed.ncbi.nlm.nih.gov/29153103/)
38. Zoller M. Tetraspanins: push and pull in suppressing and promoting metastasis. *Nat Rev Cancer* 2009; 9: 40–55. <https://doi.org/10.1038/nrc2543> PMID: [19078974](https://pubmed.ncbi.nlm.nih.gov/19078974/)
39. Yang X, Wei LL, Tang C, Slack R, Mueller S, Lippman ME. Overexpression of KAI1 suppresses in vitro invasiveness and in vivo metastasis in breast cancer cells. *Cancer Res.* 2001; 61: 5284–5288. PMID: [11431371](https://pubmed.ncbi.nlm.nih.gov/11431371/)
40. Tohami T, Drucker L, Shapiro H, Radnay J, Lishner M. Overexpression of tetraspanins affects multiple myeloma cell survival and invasive potential. *Faseb J.* 2007; 21: 691–699. <https://doi.org/10.1096/fj.06-6610com> PMID: [17210782](https://pubmed.ncbi.nlm.nih.gov/17210782/)
41. Wang X, Zhong W, Bu J, Li Y, Li R, Nie R, et al. Exosomal protein CD82 as a diagnostic biomarker for precision medicine for breast cancer. *Mol Carcinog.* 2019 Jan 3. Forthcoming.
42. Rutgen BC, Hammer SE, Gerner W, Christian M, de Arespacochaga AG, Willmann M, et al. Establishment and characterization of a novel canine B-cell line derived from a spontaneously occurring diffuse large cell lymphoma. *Leuk Res.* 2010; 34: 932–938. <https://doi.org/10.1016/j.leukres.2010.01.021> PMID: [20153049](https://pubmed.ncbi.nlm.nih.gov/20153049/)
43. Nakaichi M, Taura Y, Kanki M, Mamba K, Momoi Y, Tsujimoto H, et al. Establishment and characterization of a new canine B-cell leukemia cell line. *J Vet Med Sci.* 1996; 58: 469–471. PMID: [8741612](https://pubmed.ncbi.nlm.nih.gov/8741612/)
44. Yamazaki J, Baba K, Goto-Koshino Y, Setoguchi-Mukai A, Fujino Y, Ohno K, et al. Quantitative assessment of minimal residual disease (MRD) in canine lymphoma by using real-time polymerase chain reaction. *Vet Immunol Immunopathol.* 2008; 126: 321–331. <https://doi.org/10.1016/j.vetimm.2008.09.004> PMID: [18977540](https://pubmed.ncbi.nlm.nih.gov/18977540/)
45. Hiraoka H, Minami K, Kaneko N, Shimokawa-Miyama T, Okamura Y, Mizuno T, et al. Aberrations of the FHIT gene and Fhit protein in canine lymphoma cell lines. *J Vet Med Sci.* 2009; 71: 769–777. PMID: [19578286](https://pubmed.ncbi.nlm.nih.gov/19578286/)
46. Tomiyasu H, Goto-Koshino Y, Fujino Y, Ohno K, Tsujimoto H. Epigenetic regulation of the ABCB1 gene in drug-sensitive and drug-resistant lymphoid tumour cell lines obtained from canine patients. *Vet J.* 2014; 199: 103–109. <https://doi.org/10.1016/j.tvjl.2013.10.022> PMID: [24332606](https://pubmed.ncbi.nlm.nih.gov/24332606/)
47. Bolger AM, Lohse M, Usadel B. Trimmomatic: a flexible trimmer for Illumina sequence data. *Bioinformatics.* 2014; 30: 2114–2120. <https://doi.org/10.1093/bioinformatics/btu170> PMID: [24695404](https://pubmed.ncbi.nlm.nih.gov/24695404/)
48. Langmead B, Salzberg SL. Fast gapped-read alignment with Bowtie 2. *Nat Methods.* 2012; 9: 357–359. <https://doi.org/10.1038/nmeth.1923> PMID: [22388286](https://pubmed.ncbi.nlm.nih.gov/22388286/)
49. Robinson MD, McCarthy DJ, Smyth GK. edgeR: a Bioconductor package for differential expression analysis of digital gene expression data. *Bioinformatics.* 2010; 26: 139–140. <https://doi.org/10.1093/bioinformatics/btp616> PMID: [19910308](https://pubmed.ncbi.nlm.nih.gov/19910308/)
50. Zhou X, Lindsay H, Robinson MD. Robustly detecting differential expression in RNA sequencing data using observation weights. *Nucleic Acids Res.* 2014; 42: e91. <https://doi.org/10.1093/nar/gku310> PMID: [24753412](https://pubmed.ncbi.nlm.nih.gov/24753412/)
51. Kozomara A, Griffiths-Jones S. miRBase: annotating high confidence microRNAs using deep sequencing data. *Nucleic Acids Res.* 2014; 42: D68–73. <https://doi.org/10.1093/nar/gkt1181> PMID: [24275495](https://pubmed.ncbi.nlm.nih.gov/24275495/)
52. Kozomara A, Griffiths-Jones S. miRBase: integrating microRNA annotation and deep-sequencing data. *Nucleic Acids Res.* 2011; 39: D152–157. <https://doi.org/10.1093/nar/gkq1027> PMID: [21037258](https://pubmed.ncbi.nlm.nih.gov/21037258/)